Article

Arrays of TiO₂ Nanowires as Photoelectrochemical Sensors for Hydrazine Detection

Michael Ongaro, Michela Signoretto, Valentina Trevisan, Angela Maria Stortini and Paolo Ugo *

Department of Molecular Sciences and Nanosystems, University Ca' Foscari of Venice, Santa Marta 2137, 30123 Venice, Italy; E-Mails: michael.ongaro@unive.it (M.O.); miky@unive.it (M.S.); valentina.trevisan@unive.it (V.T.); stortini@unive.it (A.M.S.)

*   Author to whom correspondence should be addressed; E-Mail: ugo@unive.it;
    Tel.: +39-041-234-8503; Fax: +39-041-234-8594.

Abstract: Electrodes based on arrays of TiO₂ nanowires were prepared by template sol-gel synthesis with the goal of developing a hydrazine photoelectrochemical sensor. Experimental conditions were chosen so that the gelation reaction occurred inside the nanopores of track-etched polycarbonate membranes, with consequent filling with TiO₂ nanowires. Different procedures for the removal of the template were examined, in order to obtain arrays of self-standing TiO₂ nanowires. The nanowire arrays were bound to fluorine doped tin oxide substrates to produce handy photoelectrodes. The photocurrent recorded with the photoelectrodes in the presence of hydrazine showed significant dependence on the pollutant concentration. The development of a photoelectrochemical sensor for hydrazine detection in water samples, based on this principle, is presented.

Keywords: TiO₂ nanowires; hydrazine; photoelectrochemical sensor; template; environmental analysis

---

1. Introduction

In recent decades, the rapid increase in the environmental pollution has caused increasing concern for the natural ecosystems and human health. The public opinion awareness on environmental pollution led to a growing demand of analytical methods for the determination of toxic substances. Hydrazine (N_2H_4)

is an important pollutant which found wide applications in agricultural chemicals (pesticides), pharmaceutical intermediates, photographic chemicals, corrosion preserver in heat exchangers, textile dyes, fuel for rockets, spacecrafts and for emergency power unit of military aircrafts. Hydrazine is also used as precursor for the production of sodium azide, the blowing gas of car airbags. Nevertheless, hydrazine is a highly toxic material. According to the US Environmental Protection Agency, acute exposure to hydrazine can lead to temporary blindness, headache, nausea, pulmonary edema, seizures, and coma, while chronic exposure has hepatotoxic and carcinogenic effects [1]. Because of the toxicological significance of hydrazine, the development of highly sensitive and simple analytical methods for the determination of low levels of hydrazine in different samples such as drinking water and industrial effluents is highly desirable. Many methods have been proposed, these include spectrophotometry [2], titrimetry [3], chemiluminescence [4], chromatography [5] and electrochemistry [6–8].

In this work we present a new method for the determination of hydrazine, based on photoelectrochemical sensing by using a nanostructured TiO_2 photoanode. Photoelectrochemistry has been extensively used in energy harvesting and environmental decontamination [9,10], but recently it has been proposed as a promising analytical tool [11–19]. Indeed this technique has been successfully applied for the determination of environmental pollutants [14–17] and biomolecules [11–13,18,19]. Photoelectrochemical analysis employs light as the excitation source and the response in photocurrent as the detection signal; thanks to the different forms of energy use for excitation and detection, this process reduces the background signal [15]. Moreover, the instruments used for photoelectrochemical analysis are simpler and cheaper when compared with those employed for spectroscopic and chromatographic measurements.

In photocatalytic processes, TiO_2 can absorb UV photons and promote electrons (e^-) from the valence band (VB) to the conduction band (CB), leaving behind highly oxidative holes (h^+).

$$TiO_2 + h\nu \rightarrow e^- + h^+ \qquad (1)$$
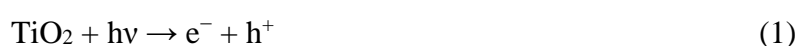
Photogenerated holes and electrons can migrate towards the surface of the TiO_2 and react with adsorbed molecules, so that e^- can take part to reduction and h^+ to oxidation reactions. Anyway, most of the photogenerated holes and electrons recombine releasing heat. However, if TiO_2 is immobilized on the surface of an electrode and an anodic potential is applied, a charge separation will be induced, so that e^- will move towards the bulk of the semiconductor and eventually to the counter electrode through the electric circuit, while the h^+ will move towards the surface of TiO_2. In this way, the recombination events are reduced and only oxidative reactions take place on the surface of the electrode. Most often, h^+ react with adsorbed water to generate hydroxyl radicals:

$$h^+ + H_2O \rightarrow {}^{\cdot}OH + H^+ \qquad (2)$$

However, the presence of easily oxidized molecules, such as hydrazine, can provide a more facile pathway for the transfer of the holes through the semiconductor/electrolyte interface, the main result being an increase of the photocurrent. The oxidation mechanism of hydrazine involves the transfer of four electrons from TiO_2, with nitrogen and four protons as products:

$$N_2H_4 + 4h^+ \rightarrow N_2 + 4H^+ \qquad (3)$$

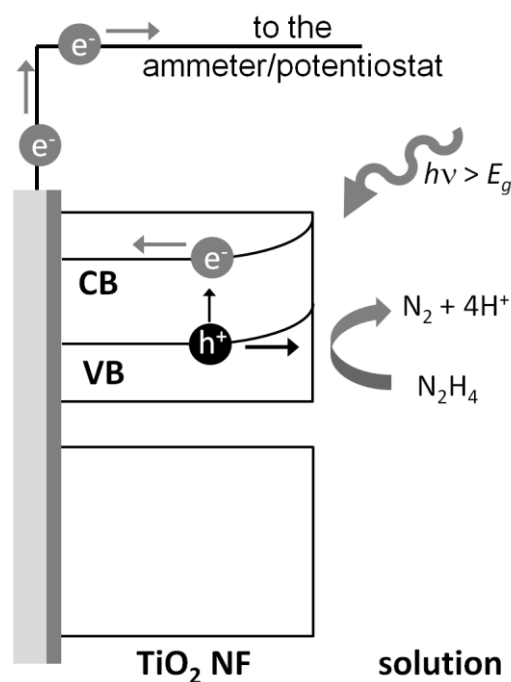The photoelectrochemical hydrazine detection mechanism at a TiO$_2$ photoanode is schematized in Figure 1.

Figure 1. Sensing scheme of hydrazine at a TiO$_2$ nanowire array (TiO$_2$NWA)photoanode; CB and VB are the semiconductor conduction and valence band.

The application of nanostructured semiconductor materials with tailored dimensions and morphology, such as nanowires (NWs), may lead to great advantages in terms of sensitivity. Quasi 1D nanostructure can provide a direct path for the collection of photogenerated electrons reducing the recombination events and consequently increasing the yield of hydrazine oxidation [20]. Moreover, NW based electrodes own a larger surface area with respect to planar electrodes, increasing the area of the electrolyte/semiconductor interface and the overall photoelectrochemical reaction rate [21]. On this basis we used a recently developed sol-gel template method [22] for the synthesis of TiO$_2$NWs which were used for the fabrication of a photoelectrochemical sensor. The sensor gave promising results in the photoelectrochemical determination of hydrazine in water.

2. Experimental Section

2.1. Chemicals and Materials

All the chemicals employed were of reagent grade quality and used without further purification. Polycarbonate track-etched membranes (pore diameter 200 nm, pore density 3×10^8 pores/cm^2, membrane thickness 10 μm) were purchased from *Osmonic Inc*. Fluorine doped tin oxide (FTO) transparent electrodes (7 Ω/sq) were purchased from *Solaronix*.

2.2. Template Synthesis

15 mL of titanium tetraisopropoxide (TTiP) were mixed to 30 mL of ethanol. In a different becker, 5.26 mL of acetilacetone (AcAc) and 2.72 mL of distilled water were mixed to 30 mL of ethanol. Then the first solution was poured, drop by drop, on the second solution and stirred at room temperature for 2 h. The molar composition of the final bath is TTiP/H_2O/AcAc/EtOH = 1/3/1/20. Track-etched polycarbonate membranes were used as templating material. A fraction of about 20 mL of the yellow colored sol was pumped through the membrane (placed in a filter-holder) using a syringe. The pumping procedure was repeated 8–10 times. In the mean time the residual sol was taken to boiling temperature. After the pumping process, the membrane was immersed in the boiling sol for 20 min. Subsequently, the membrane was removed from the bath and dried overnight at room temperature before heating in an oven for three hours at 100 ℃ at stationary regime.

2.3. Electrodes Fabrication

FTO transparent electrodes were cleaned by sonication for 30 min in isopropanol and 30 min in deionized water before use.

For the preparation of the array of TiO_2 nanowires (TiO$_2$NWA), a drop of TTiP was casted on the conductive side of a FTO slide (about 0.7 cm^2) and a square shaped piece (about 0.25 cm^2) of TiO_2 filled polycarbonate membrane was placed over it. The FTO slide was placed in an oven at 200 ℃ for one hour in order to allow the membrane to adhere to the FTO substrate. Subsequently the electrode was immersed in CH_2Cl_2 for 30 min in order to dissolve the polycarbonate template, obtaining a free standing array of NWs attached to the FTO. Finally, the electrode was calcined at 450 ℃ in flow air (30 mL/min) for 3 h. Eventual flat residuals of titania on top of TiO$_2$-NW can be removed by reactive plasma etching with CF_4.

A strip of copper tape with conductive glue was used to create the electrical contact and a strip of Kapton® tape with a circular hole was used to define the final geometric area of the electrode, namely 0.07 cm^2.

2.4. Sensor Characterizations

SEM-EDX analyses were performed with a HITACHI TM3000 and a JEOL JSM-5600LV equipped with a Vega LVM TESCAN energy-dispersive X-ray spectrometer.

2.5. Photoelectrochemical Hydrazine Determination

The TiO$_2$NWA electrode was used for the photoelectrochemical determination of hydrazine in water. All the photoelectrochemical analyses were performed using a CHi 660 b potentiostat, in a three electrodes quartz cell. An Ag/AgCl (KCl saturated electrode) was used as reference electrode and a platinum coil was used as counter electrode. UV light irradiation was performed using three 'TL' 20W/05 PHILIPS UV-lamps.

Amperometric I-t curves were recorded applying a constant potential of 0.400 V in 0.1 M phosphate buffer (PB) solution pH 7.0. The current was measured for the first thirty seconds in the dark, then the lamps were turned on and the electrode was irradiated with UV light.

3. Results and Discussion

3.1. Electrode Fabrication

The procedure for the sol-gel template synthesis of TiO$_2$NW has been already presented in a previous work [22] and therefore it will be discussed here only briefly.

Metal-alkoxides, which are common precursors in sol-gel synthesis, are very reactive, making the pores filling process rather critical. Indeed, if the sol-gel reaction is too fast, the pores of the membrane could be blocked by large gel particles generated in the bulk of the solution, preventing the formation of a continuous metal oxide network within the pores. On the other hand, an equimolar mixture of TTiP and AcAc is stable for several hours, this allowed us to use a syringe to push the suspension inside the pores of the membrane, which was previously placed inside a membrane holder. Subsequently, the sol filled membrane was allowed to dry over night at room temperature and in an oven for three hours at 100 ℃. At this point, the membrane was dissolved in an organic solvent, namely CH$_2$Cl$_2$, without damaging the TiO$_2$NW. Figure 2 shows the SEM images of the TiO$_2$NWA after the dissolution of the templating membrane. Free standing NWs of 200 nm in diameter and about 8 μm in length can be clearly seen. These dimensions are in good agreement with the pore diameter and with the thickness of the templating membrane which are 200 nm and 10 μm respectively.
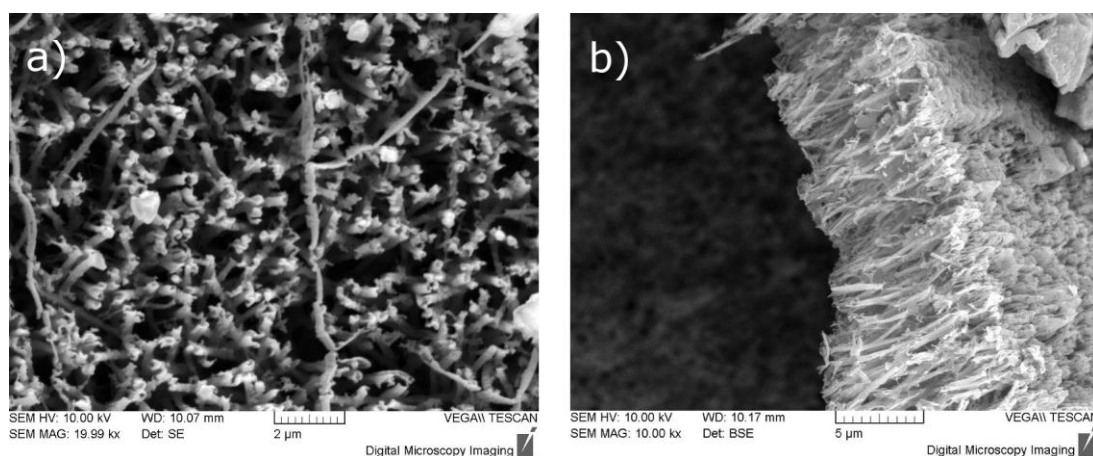

Figure 2. SEM image of a TiO$_2$NWA (**a**) top-view; (**b**) lateral view.

After removing the template, the array was immobilized on the surface of the FTO electrode and heated at 450 ℃ for three hours. The thermal treatment is important in order to remove the organic ligand still present in the TiO$_2$ framework and to induce the crystallization of amorphous TiO$_2$ to anatase [22], which is the most photoactive crystal habit [23]. Further information concerning the characterization of the TiO$_2$NWA can be found in a recent publication [22].

3.2. Influence of Bias Potential on the Hydrazine Determination

The analytical response of the sensor was recorded as anodic photocurrent, calculated as the difference between the current recorded in the dark and under UV irradiation, when a constant positive bias is applied. The bias potential is an important parameter in the photoelectrochemical hydrazine oxidation process. In order to determine the best anodic potential, we recorded a linear sweep

voltammetry (LSV) at low scan rate (5 mV s^{-1}) under chopped light, in 0.1 M phosphate buffer (PB) solution, pH 7.0, 0.1 mM hydrazine, using a TiO$_2$NWA as the working electrode. By this way a voltammogram was obtained in which both photocurrent and current in the dark are recorded on a large potential window, namely from −0.5 V to 0.8 V *vs.* Ag/AgCl. For each step in Figure 3, the upper part of the signal is the photocurrent, the lower is the current recorded in the dark.
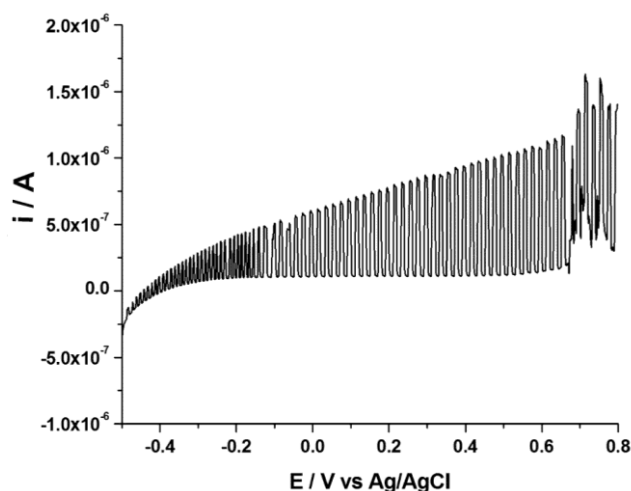

Figure 3. Linear sweep voltammetry recorded in 0.1 M phosphate buffer, pH 7, 0.1 mM hydrazine under chopped UV light. WE: TiO$_2$NWA; RE: Ag/AgCl (KCl saturated; CE: Platinum Coil, scanrate 5 mV s^{-1}.

The voltammogram shows that 0.4 V is the optimal bias, as the photocurrent reaches its highest value while practically no faradic process is active in the dark, such processes become relevant at potentials more positive than 0.5 V.

3.3. Photoelectrochemical Determination of Hydrazine

Amperometric i-t measurements were used to study the photoelectrochemical response of the TiO$_2$NWA sensor to hydrazine concentration. A typical analysis is reported in Figure 4. The first 30 s of the scan are recorded in the dark; during this time an anodic current is detected, which is ascribed to the formation of the space charge region on the TiO$_2$. After this time, upon irradiation with UV light, a strong increase in the anodic current is observed. The photocurrent pattern can be divided into two phases. At the beginning of the irradiation, a steep increase of the photocurrent is observed generating a peak shaped curve, subsequently the photocurrent decreases up to reaching a steady state. This behavior is typical for TiO$_2$ photoelectrodes and it is described as a classical onset of recombination [24,25]. The polarization step in the dark is important in order to allow the proper build-up of the space charge region which is responsible for the separation of the photogenerated charges, allowing to increase the photocurrent and, consequently, the analytical signal. Anyway, since the current measured under irradiation includes the current related to the photoelectrochemical oxidation at the semiconductor electrode plus the double layer and space charge region charging current, the analytical signal (i_{ph}) was calculated as the difference between the mean current value recorded during the last 3 s in the dark and the mean value of the photocurrent recorded during the last 3 s of the analysis under UV irradiation.
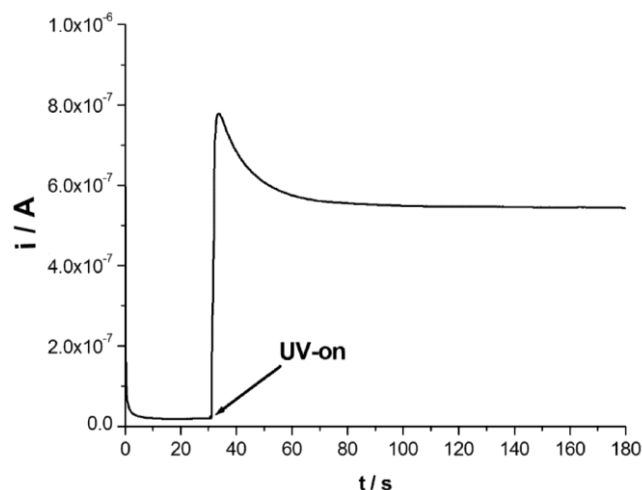
Figure 4. Amperometric i-t curve recorded at the TiO_2NWA applying a potential step at + 0.4 V vs Ag/AgCl in 0.1 M phosphate buffer, pH 7.0, 10 μM hydrazine. UV irradiation is turned on after 30 s from the beginning of the analysis.

This protocol has been used for the determination of different concentrations of hydrazine in the range of 0–1000 μM. Three repeated measurements were performed for each hydrazine concentration. The mean photocurrent values have been plotted against the logarithm of the hydrazine concentration. The calibration plot is linear over a wide range (up to 1×10^{-3} M) and can be expressed by the equation $i_{ph}[A] = 3.0 \times 10^{-7} \cdot logC \cdot [log \mu M] + 2.06 \times 10^{-7}$, with a correlation coefficient of 0.9919 (Figure 5). The limit of detection (LOD) is 1.91 μM, calculated as $LOD = 3\sigma_b/m$, where σ_b is the blank standard deviation and m is the sensitivity (slope of the calibration plot). The quantification limit (LOQ), calculated as $LOQ = 10\sigma_b/m$, is 8.91 μM.
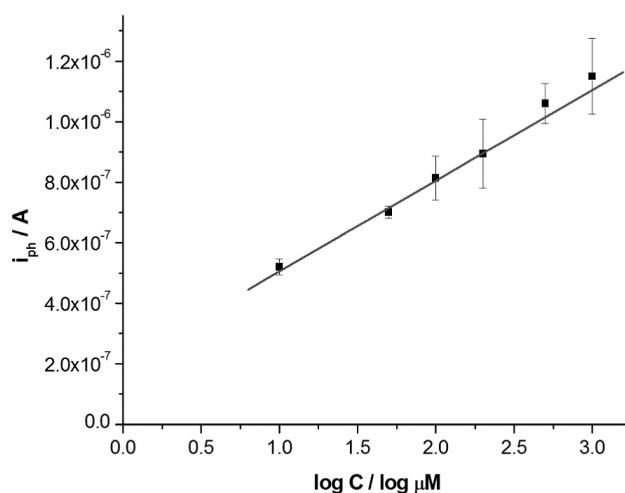

Figure 5. Plot of photocurrent as a function of logarithm of hydrazine concentration.

These results confirm that the photoelectrochemical determination of hydrazine can be a readily performed with templated TiO_2 nanowires. Table 1 compares the analytical parameters obtained here with those previously achieved with other methods.

Table 1. Comparison of some of the analytical parameters of the different methods for hydrazine determination.

Method	Electrode	LOD (μM)	Reference
Chromatography	//	0.03	[5]
Spectrophotometry	//	30* (45)	[2]
Chemiluminescence	//	0.5* (0.75)	[4]
Electrocatalysis	NPHMGC[a]	8	[5]
Electrocatalysis	PCVMGC[b]	4.2	[6]
Electrocatalysis	NHCFMGC[c]	90.6	[7]
Electrocatalysis	MNPMBDD[d]	1–3.27	[26–28]
Photoelectrochemistry	Ti/TiO$_2$[e]	8.54	[13]
Photoelectrochemistry	TiO$_2$NWA	1.91	present work

[a] Nickel hexacyanoferrate nanoparticles modified carbon ceramic electrode; [b] Pyrocatechol violet modified glassy carbon electrode; [c] Nickel hexacyanoferrate nanoparticles modified graphite electrode; [d] Metal nanoparticles modified boron doped diamond electrodes; [e] Anodized titania. * LOD calculated as 2σ, in parenthesis as 3σ.

It can be seen that, among electrochemical methods, only those which employed metal nanoparticles modified boron doped diamond electrodes (MNPMBDD) [26–28] gave LODs comparable with the one achieved with the present TiO$_2$NWA; it is worth to note that the modification of BDD with noble metals nanoparticles is however complex and require expensive materials. TiO$_2$NWA allowed us to get improved LOD also with respect to the other photoelectrochemical method based on flat TiO$_2$ photoanodes. This demonstrates that the use of nanostructured materials improves the analytical performances of the photoelectrochemical sensor. Chromatographic methods achieved lower LOD, but these analytical procedures require complex pretreatments of the samples, including a hydrazine derivatization reaction, which makes these methods less practical, more expensive and time consuming. Flow injection with chemiluminescence detection also furnished a very low LOD [4], however with a linearity limit which extends only to 5×10^{-5} M *vs.* 1×10^{-3} M for our method.

4. Conclusions

Based on the data presented here, it can be concluded that photoelectrochemistry is a promising method for the determination of hydrazine. TiO$_2$NWA based sensors showed satisfactory linearity range and detection limit when compared to other methods reported in literature. We also demonstrated that the performances of photoelectrochemistry based methods can be improved by tailoring the morphology of the photoanode, indeed, by using structures based on TiO$_2$ nanowires, the electron-hole recombination process can be decreased resulting in an increase of the analytical signal. Further improvements could be achieved by functionalizing the semiconductor with electrocatalytic nanoparticles, in order to improve the reaction rate and the charge separation efficiency. Since this sensor, in principle, can work with other oxidizable organic species, further studies will aim to extend the applicability of this method to other relevant organic environmental pollutants.

Acknowledgments

Author Contributions

M.O. and P.U. conceived and designed the experiments; M.O. performed the experiments; M.O and P.U. analyzed the data; M.S. and V.T. contributed reagents and materials; A.S. performed analysis; M.O and P.U. wrote the paper.

Conflicts of Interest

The authors declare no conflict of interest.

References

1. United States Environmental Protection Agency. Hydrazine Hazard Summary-Created in April 1992; Revised in January 2000. Available online: http://www.epa.gov/ttnatw01/hlthef/hydrazin.html (accessed on 6 May 2015).
2. Safavi, A.; Ensafi, A.A. Kinetic spectrophotometric determination of hydrazine. *Anal. Chim. Acta* **1995**, *300*, 307–311.
3. Rajasekharan, V.; Ramachandran, C.G. The titration of isoniazid and other hydrazine derivatives with chloramine-t. *Anal. Chim. Acta* **1971**, *57*, 429–434.
4. Safavi, A.; Baezzat, M.R. Flow injection chemiluminescence determination of hydrazine. *Anal. Chim. Acta* **1998**, *358*, 121–125.
5. Evgen'ev, M.I.; Evgen'eva, I.I.; Ismailova, R.N. Extraction-chromatographic determination of hydrazine in natural water as a 5,7-dinitrobenzofurazan derivative using diode-array detection. *J. Anal. Chem.* **2000**, *55*, 933–937.
6. Abbaspour, A.; Khajehzadeh, A.; Ghaffarinejad, A. Electrocatalytic oxidation and determination of hydrazine on nickel hexacyanoferrate nanoparticles-modified carbon ceramic electrode. *J. Electroanal. Chem.* **2009**, *631*, 52–57.
7. Golabi, S.M.; Zare, H.R.; Hamzehloo, M. Electrocatalytic oxidation of hydrazine at a pyrocatechol violet (PCV) hemically modified electrode. *Microchem. J.* **2001**, *69*, 13–23.
8. Shankaran, D.R.; Narayanan, S.S. Amperometric sensor for hydrazine determination based on mechanically immobilized nickel hexacyanoferrate modified electrode. *Russ. J. Electrochem.* **2001**, *37*, 1149–1153.
9. Liu, S.; Liu, B.; Nakata, K.; Ochiai, T.; Murakami, T.; Fujishima, A. Electrospinning preparation and photocatalytic activity of porous TiO_2 nanofibers. *J. Nanomater.* **2012**, *2012*, doi:10.1155/2012/491927.
10. Reddy, K.R.; Nakata, K.; Ochiai, T.; Murakami, T.; Tryk, D.A.; Fujishima, A. Facile fabrication and photocatalytic application of Ag nanoparticles-TiO_2 nanofiber composites. *J. Nanosci. Nanotechnol.* **2011**, *11*, 3692–3695.

11. Haddour, N.; Chauvin, J.; Gondran, C.; Cosnier, S. Photoelectrochemical immunosensor for label-free detection and quantification of anti-cholera toxin antibody. *J. Am. Chem. Soc.* **2006**, *128*, 9693–9698.

12. An, Y.; Tang, L.; Jiang, X.; Chen, H.; Yang, M.; Jin, L.; Zhang, S.; Wang, C.; Zhang, W. A photoelectrochemical immunosensor based on Au-doped TiO_2 nanotube arrays for the detection of α-synuclein. *Chem. Eur. J.* **2010**, *16*, 14439–14446.

13. Tu, W.; Lei, J.; Wang, P.; Ju, H. Photoelectrochemistry of free-base-porphyrin-functionalized zinc oxide nanoparticles and their applications in biosensing. *Chem. Eur. J.* **2011**, *17*, 9440–9447.

14. An, X.; Teng, F.; Zhang, P.; Zhao, C.; Pan, X.; Zhang, Z.; Xie, E. Enhanced photoelectrochemical sensor based on $ZnO–SnO_2$ composite nanotubes. *J. Alloy. Compd.* **2014**, *614*, 373–378.

15. Ojani, R.; Zarei, E. A new simple electrochemically assisted photocatalysis sensor of hydrazine using Ti/TiO_2 electrode. *J. Braz. Chem. Soc.* **2013**, *24*, 657–662.

16. Hu, Y.; Xue, Z.; He, H.; Ai, R. Liu, X.; Lu, X. Photoelectrochemical sensing for hydroquinone based on porphyrin-functionalized Au nanoparticles on grapheme. *Biosens. Bioelectron.* **2013**, *47*, 45–49.

17. Rajeshwar, K. Photoelectrochemistry and the environment. *J. Appl. Electrochem.* **1995**, *25*, 1067–1082.

18. Zhang, X.; Guo, Y.; Liu, M.; Zhang, S. Photoelectrochemically active species and photoelectrochemical biosensors. *RSC Adv.* **2013**, *3*, 2846–2857.

19. Voccia, D.; Palchetti, I. Photoelectrochemical biosensors for nucleic acid detection. *J. Nanosci. Nanotechnol.* **2015**, *15*, 3320–3332.

20. Law, M.; Greene, L.E.; Johnson, J.C.; Saykally, R.; Yang, P. Nanowire dye-sensitized solar cells. *Nat. Mater.* **2005**, *4*, 455–459.

21. Ongaro, M.; Gambirasi, A.; Favaro, M.; Ugo, P. Electrochemical synthesis and characterization of hierarchically branched ZnO nanostructures on ensembles of gold nanowires. *Electrochim. Acta* **2012**, *78*, 539–546.

22. Ongaro, M.; Mardegan, A.; Stortini, A.M.; Signoretto, M.; Ugo, P. Arrays of templated TiO_2 nanofibres as improved photoanodes for water splitting under visible light. *Nanotechnology* **2015**, *26*, 165402.

23. Signoretto, M.; Ghedini, E.; Pinna, F.; Nichele, V.; Crocella, V.; Cerrato, G. Effect of textural properties on the drug delivery behaviour of nanoporous TiO_2 matrices. *Microporous Mesoporous Mater.* **2011**, *139*, 189–196.

24. Ghicov, A.; Schmidt, B.; Kunze, J.; Schmuki, P. Photoresponse in the visible range from Cr-doped TiO_2 nanotubes. *Chem. Phys. Lett.* **2007**, *433*, 323–326.

25. Spadavecchia, F.; Ardizzone, S.; Cappelletti, G.; Falciola, L.; Ceotto, M.; Lotti, D. Investigation and optimization of photocurrent transient measurements on nano-TiO_2. *J. Appl. Electrochem.* **2013**, *43*, 217–225.

26. Channon, R.B.; Newland, J.C.; Bristow, A.W.T.; Ray, A.D.; Macpherson, J.V. Selective detection of hydrazine in the presence of excess electrochemically active pharmaceutical ingredients using boron doped diamond metal nanoparticle functionalised electrodes. *Electroanalysis* **2013**, *25*, 2613–2619.

27. Sun, H.; Dong, L.; Yu, H.; Huo, M. Direct electrochemical oxidation and detection of hydrazine on a boron doped diamond (BDD) electrode. *Russ. J. Electrochem.* **2013**, *49*, 883–887.

28. Batchelor-McAuley, C.; Banks, C.E.; Simm, A.O.; Jones, T.G.J.; Compton, R.G. The electroanalytical detection of hydrazine: A comparison of the use of palladium nanoparticles supported on boron-doped diamond and palladium plated BDD microdisc array. *Analyst* **2006**, *131*, 106–110.